Ocean Modelling 172 (2022) 101976

Contents lists available at ScienceDirect

Ocean Modelling

journal homepage: www.elsevier.com/locate/ocemod

The impact of ocean biogeochemistry on physics and its consequences for modelling shelf seas

Jozef Skákala [a,b,*], Jorn Bruggeman [c,a], David Ford [d], Sarah Wakelin [e], Anıl Akpınar [e], Tom Hull [f,g], Jan Kaiser [g], Benjamin R. Loveday [h], Enda O'Dea [d], Charlotte A.J. Williams [e], Stefano Ciavatta [a,b]

[a] Plymouth Marine Laboratory, Prospect Place, The Hoe, Plymouth, PL1 3DH, United Kingdom
[b] National Centre for Earth Observation, Prospect Place, The Hoe, Plymouth, PL1 3DH, United Kingdom
[c] Bolding & Bruggeman ApS, Strandgyden 25, Asperup, 5466, Denmark
[d] Met Office, FitzRoy Road, Exeter, EX1 3PB, United Kingdom
[e] National Oceanography Centre, Joseph Proudman Building, 6 Brownlow Street, Liverpool, L3 5DA, United Kingdom
[f] Centre for Environment, Fisheries and Aquaculture Science, Lowestoft, NR33 0HT, United Kingdom
[g] Centre for Ocean and Atmospheric Science, University of East Anglia, Norwich, NR4 7TJ, United Kingdom
[h] Innoflair UG, Richard-Wagner-Weg 35, Darmstadt, 64287, Germany

ARTICLE INFO

Keywords:
Impact of biogeochemistry on physics
Two-way coupled physical–biogeochemical model
Ocean chlorophyll concentration
Sea surface temperature
Phytoplankton spring bloom
North-West European Shelf (10E–10W, 40N–68N)
Data assimilation
Operational systems

ABSTRACT

We use modelling and assimilation tools to explore the impact of biogeochemistry on physics in the shelf sea environment, using North-West European Shelf (NWES) as a case study. We demonstrate that such impact is significant: the attenuation of light by biogeochemical substances heats up the upper 20 m of the ocean by up to 1 °C and by a similar margin cools down the ocean within the 20–200 m range of depths. We demonstrate that these changes to sea temperature influence mixing in the upper ocean and feed back into marine biology by influencing the timing of the phytoplankton bloom, as suggested by the critical turbulence hypothesis. We compare different light schemes representing the impact of biogeochemistry on physics, and show that the physics is sensitive to both the spectral resolution of radiances and the represented optically active constituents. We introduce a new development into the research version of the operational model for the NWES, in which we calculate the heat fluxes based on the spectrally resolved attenuation by the simulated biogeochemical tracers, establishing a two-way coupling between biogeochemistry and physics. We demonstrate that in the late spring–summer the two-way coupled model increases heating in the upper oceanic layer compared to the existing model and improves by 1–3 days the timing of the simulated phytoplankton bloom. This improvement is relatively small compared with the existing model bias in bloom timing, but is sufficient to have a visible impact on model skill in the free run. We also validate the skill of the two-way coupling in the context of the weakly coupled physical–biogeochemical assimilation currently used for operational forecasting of the NWES. We show that the change to the skill is negligible for analyses, but it remains to be seen how much it differs for the forecasts.

1. Introduction

Within the Earth system, physics and biology mutually interact in many non-trivial ways. In the marine environment biological processes are driven by physical transport, mixing, temperature, salinity and the incoming light, whereas biology impacts physics through its role in the carbon cycle (microbial and biological pump, e.g. Riebesell et al. (2009)), oceanic albedo (Jin et al., 2004), underwater light attenuation (Morel, 1988; Simonot et al., 1988; Sathyendranath et al., 1991; Edwards et al., 2004; Oschlies, 2004; Manizza et al., 2005; Marzeion et al., 2005; Sweeney et al., 2005; Lengaigne et al., 2007; Jochum et al., 2010; Zhai et al., 2011; Turner et al., 2012), and its influence on cloud condensation nuclei through the production of dimethyl sulphide (DMS, Lovelock et al. (1972), Charlson et al. (1987), Six et al. (2013), Schwinger et al. (2017)), or through bubble formation (Wilson et al., 2015). While the impact of physics on biology is never neglected or disputed, the impact of biology on physics became often a matter of controversy, for example in connection with "the Gaia hypothesis" (Lovelock, 1979, 2000), which proposes that life plays a central role in regulating climate. Marine model development largely reflects this underlying scientific attitude, i.e. the common way to simplify complex coupled physical–biogeochemical dynamics is to neglect the impact of the simulated biogeochemistry on physics (Heinze and Gehlen, 2013; Gehlen et al., 2015; Ford et al., 2018), so that the physical component

* Corresponding author at: Plymouth Marine Laboratory, Prospect Place, The Hoe, Plymouth, PL1 3DH, United Kingdom.
E-mail address: jos@pml.ac.uk (J. Skákala).

https://doi.org/10.1016/j.ocemod.2022.101976
Received 12 April 2021; Received in revised form 22 December 2021; Accepted 4 February 2022
Available online 18 February 2022
1463-5003/Crown Copyright © 2022 Published by Elsevier Ltd. This is an open access article under the CC BY license (http://creativecommons.org/licenses/by/4.0/).

can be run entirely independently of the biogeochemical model (we will further call such models "one-way coupled").

The most obvious source of biogeochemical feedback to physics in coupled physical–biogeochemical ocean models is the attenuation of underwater radiances by optically active biogeochemical tracers and the subsequent impact on heat fluxes, temperature and mixed layer depth (MLD). One-way coupled models either do not represent this effect at all, or they incorporate it "offline" based on external forcing, such as using observational products for surface diffuse attenuation coefficients (e.g. Madec et al. (2015)). However, since our overall goal is to realistically represent environmental processes, or to produce reliable global climate projections, it is a matter of importance to better understand both the biogeochemical impact on ocean physics, and the sensitivity of the simulated physics to how precisely such an impact is incorporated into the physical model. Only by answering these two questions can we see to what extent the simplifications usually adopted in our models are justified.

Studies have looked at the impact of biogeochemical light attenuation on marine physics, e.g in the North Atlantic (Oschlies, 2004), tropical Pacific (Lengaigne et al., 2007) and globally (Manizza et al., 2005), demonstrating that the impact can be substantial, but regionally-dependent. However, the studies so far largely focused on the open ocean that dominates the global scales, and there is a lack of a more detailed study of such impact in the shelf sea environment. Shelf seas are highly productive parts of the ocean (Borges et al., 2006; Jahnke, 2010), which makes them particularly relevant to study the complex interaction between biogeochemistry and physics. In this study we will employ state-of-the-art modelling tools (e.g. Skákala et al. (2020)) to estimate the impact of biogeochemical tracers on vertical light and heat attenuation on the North-West European Shelf (NWES), a region of particular interest for the European economy (Pauly et al., 2002) and carbon cycle (Borges et al., 2006; Jahnke, 2010). Furthermore, we will determine how sensitive the physical model of the NWES is to the adopted light scheme used to drive the heat fluxes in the water column.

As part of the work described in this study we implemented, into the physical model within a research version of the Copernicus Marine Environment Monitoring Service (CMEMS) operational system for the NWES, a state-of-the-art representation of underwater radiances. This uses the spectrally resolved bio-optical module from Skákala et al. (2020), based on the OASIM model of Gregg and Casey (2009). Since the attenuation in the newly implemented module is calculated using the simulated biogeochemical tracers, the physics now depends on the simulated biogeochemistry (henceforth, we will refer to such models as "two-way coupled", for examples see Oschlies (2004), Manizza et al. (2005), Lengaigne et al. (2007)). We will provide a detailed evaluation of the updated system performance including the weakly coupled physical–biogeochemical data assimilation. The aim of this evaluation is to provide a recommendation of whether the new set-up should be considered for operational use.

A specific problem of focus for this study is the impact of the changed physics (within the newly introduced two-way coupled model) on the simulated biogeochemistry. The existing CMEMS operational system is one-way coupled, and it has been argued (Skákala et al., 2020) that it may be underestimating the heating in the upper ocean, at least relative to the newly introduced two-way coupled model. The expected increase in upper-ocean heating due to two-way coupling is likely to reduce convective mixing in the upper ocean (Taylor and Ferrari, 2011; Smyth et al., 2014), which may change the timing of the spring phytoplankton bloom, as per the critical turbulence hypothesis (Huisman et al., 1999; Waniek, 2003). To be more specific: although many factors can influence the bloom timing (including biological drivers, such as zooplankton grazing, e.g. Behrenfeld and Boss (2018)), the critical turbulence hypothesis is one of the leading hypotheses for how blooms are triggered in the North Atlantic, suggesting that the bloom happens when the effective mixing depth is fully contained within the lit layer. Reducing convective mixing can then reduce the effective mixing depth and trigger an earlier phytoplankton bloom (for the mechanism see the schematic in Fig. 1), which would be desirable, as the current operational model is known to produce late and intense spring blooms (Skákala et al., 2020, 2021). Since a spring bloom is a major ecosystem driver on the NWES (Lutz et al., 2007; Henson et al., 2009), any improvements in bloom timing could have an important knock-on effect on the biogeochemical model skill.

The questions outlined in this study will be addressed by analysing outputs of a number of suitably designed free and assimilative runs. The paper will be structured as follows: Firstly we will describe the model, light scheme and, if present, the assimilation set-up for the different simulations, as well as the methodology on how to validate and compare those different simulations. This will be followed by the section describing the results on the sensitivity of temperature to the light attenuation by the biogeochemical tracers, as well as to the adopted light scheme, and also on the impact of two-way coupling and assimilation on the coupled physical–biogeochemical model skill. In the last part we will discuss our results and outline the directions for future research.

2. Methods

2.1. The physical model: Nucleus for European Modelling of the Ocean (NEMO)

The NEMO ocean physics component (OPA) is a finite difference, hydrostatic, primitive equation ocean general circulation model (Madec et al., 2015). The NEMO configuration used in this study is similar to the one used by Ford et al. (2017), Skákala et al. (2018, 2020), and identical to the configuration used in Skákala et al. (2021): we use the CO6 NEMO version, based on NEMOv3.6, a development of the CO5 configuration explained in detail by O'Dea et al. (2017). The model has 7 km spatial resolution on the Atlantic Margin Model (AMM7) domain using a terrain-following $z^*-\sigma$ coordinate system with 51 vertical levels (Siddorn and Furner, 2013). The lateral boundary conditions for physical variables at the Atlantic boundary were taken from the outputs of the Met Office operational 1/12° North Atlantic model (NATL12, Storkey et al. (2010)); the Baltic boundary values were derived from a reanalysis produced by the Danish Meteorological Institute for CMEMS. We used river discharge based on data from Lenhart et al. (2010). The model was forced at the surface by atmospheric fluxes provided by an hourly and 31 km resolution realization (HRES) of the ERA5 data-set (https://www.ecmwf.int/).

This paper compares several light schemes previously used in the literature to calculate the NEMO oceanic heat fluxes (for the summary see Table 1):

(i) The existing reanalysis version of the operational one-way coupled model (e.g. Skákala et al. (2018)), which takes the total incoming net shortwave radiation from the ERA5 data, splits it into visible (400–700 nm) and invisible fractions, with the visible fraction attenuated inside the water column based on the K_d for 490 nm wavelength supplied by a monthly climatology from an Ocean Color - Climate Change Initiative (OC-CCI) product of European Space Agency (ESA), version 4.1 (https://www.esa-oceancolour-cci.org/), and the invisible waveband attenuated with a constant e-folding depth of 0.35 m.

(ii) The red–green–blue (RGB) scheme by Lengaigne et al. (2007), which uses the visible fraction of light spectrally resolved into 3 wavebands: blue (400–500 nm), green (500–600 nm) and red (600–700 nm) and attenuates it by the sea water and phytoplankton chlorophyll. By default, chlorophyll is taken to be a constant 0.05 mg/m^3, a minimal value representative of oligotrophic waters, as in Lengaigne et al. (2007), O'Dea et al. (2017), Graham et al. (2018). Alternatively, chlorophyll can be simulated by a biogeochemical model, as in Lengaigne et al. (2007). Both these chlorophyll schemes will be included into our study.

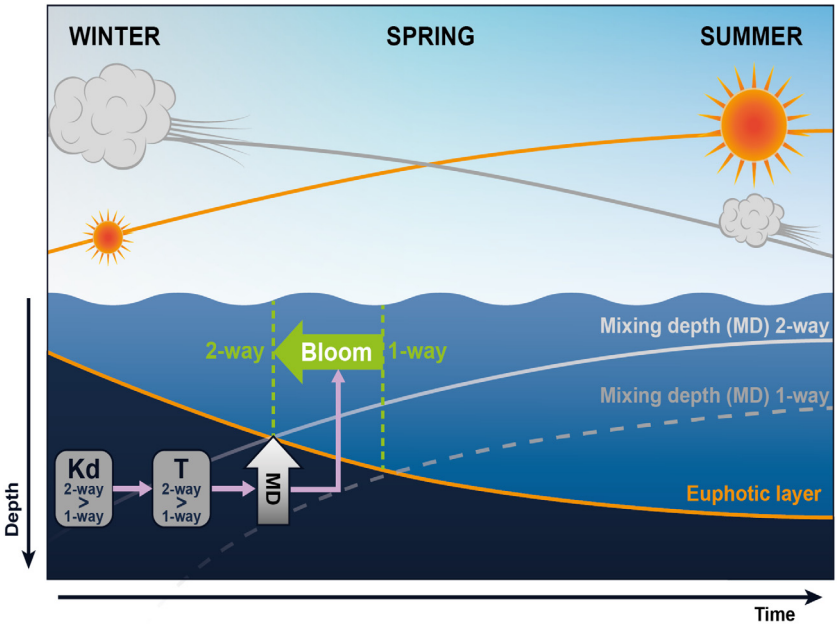

Fig. 1. A schematic representation of the hypothesis about the impact of the two-way coupled model on the timing of the simulated bloom.

(iii) The two-way coupled run using the implementation of a bio-optical module based on the OASIM model (Gregg and Casey, 2007; Gregg and Rousseaux, 2016; Skákala et al., 2020), providing spectrally (in 33 wavebands) resolved radiance decomposed into direct and diffuse streams. For a detailed description of the bio-optical module and the attenuation scheme see the next section describing the European Regional Seas Ecosystem Model (ERSEM) model.

(iv) We will also use the scheme based on the bio-optical module to simulate the attenuation by clear water-only, to provide a baseline run for the comparison of how biology and the different light schemes impact physics on the NWES.

In each of the previous cases, the underwater radiances are at every vertical level integrated by NEMO to calculate the heating within each vertical layer as

$$\frac{dT}{dt} = \frac{dI}{dz} \cdot \frac{1}{C\rho}, \tag{1}$$

where T is temperature, t is time, dI is, for each vertical model layer, the difference between the irradiance penetrating the top of a grid box and that leaving the bottom, dz is the vertical distance between the top and bottom of the grid box, C is heat capacity and ρ is the reference water density.

2.2. The ecosystem model: the European Regional Seas Ecosystem Model (ERSEM)

ERSEM (Baretta et al., 1995; Butenschön et al., 2016; Marine Systems Modelling Group, 2020) is a lower trophic level ecosystem model for marine biogeochemistry, pelagic plankton, and benthic fauna (Blackford, 1997). In this study, ERSEM is coupled to the physical model NEMO using Framework for Aquatic Biogeochemical Models (FABM, Bruggeman and Bolding (2014, 2020)). ERSEM splits phytoplankton into four functional types largely based on their size (Baretta et al., 1995): picophytoplankton, nanophytoplankton, diatoms and dinoflagellates. ERSEM uses variable stoichiometry for the simulated plankton groups (Geider et al., 1997; Baretta-Bekker et al., 1997) and each Phytoplankton Functional Type (PFT) biomass is represented in terms of chlorophyll, carbon, nitrogen and phosphorus, with diatoms also represented by silicon. ERSEM predators are composed of three zooplankton types (mesozooplankton, microzooplankton and heterotrophic nanoflagellates), with organic material being decomposed by one functional type of heterotrophic bacteria (Butenschön et al., 2016). The ERSEM inorganic component consists of nutrients (nitrate, phosphate, silicate, ammonium and carbon) and dissolved oxygen. The carbonate system is also included in the model (Artioli et al., 2012).

We applied in this study the ERSEM configuration from Skákala et al. (2021), based on a new ERSEM version 20.10, which has an updated benthic component with respect to Butenschön et al. (2016). The ERSEM parametrization is identical to the one described in Butenschön et al. (2016). The Atlantic boundary values for nitrate, phosphate, silicate and oxygen were taken from World Ocean Atlas (Garcia et al., 2013) and dissolved inorganic carbon from the GLODAP gridded dataset (Key et al., 2015; Lauvset et al., 2016), while plankton and detritus variables were set to have zero fluxes at the Atlantic boundary.

The irradiance at the ocean surface was calculated for all the runs using the bio-optical module implemented into the NEMO-FABM-ERSEM AMM7 configuration by Skákala et al. (2020). The bio-optical module resolves irradiance spectrally (33 wavebands in the 250–3700 nm range) and distinguishes between downwelling direct and diffuse streams. The module is forced by the ERA5 atmospheric inputs (https://www.ecmwf.int/) for total vertically integrated ozone, water vapour, cloud cover, cloud liquid water and sea-level air pressure, as well as by a satellite product for aerosol optical thickness (MODerate resolution Imaging Spectroradiometer, MODIS, https://modis.-gsfc.nasa.gov/data/dataprod), and also by data for surface wind speed, air humidity, and air temperature, all provided by the NEMO atmospheric (ERA5) forcing. The attenuation of the irradiance was described in detail by Gregg and Rousseaux (2016), Skákala et al. (2020), here it is briefly summarized: The module distinguishes between the absorption and scattering by the sea water and the 4 PFTs, based on the wavelength-dependent absorption, total scattering and backscattering coefficients from Gregg and Rousseaux (2016). Although we included the impact of backscattering on the light attenuation, similarly to Skákala et al. (2020), we argue that explicitly tracking the upwelling stream can be reasonably neglected. Besides the clear sea water and PFTs, we included into the light attenuation also the absorption by POM, CDOM and sediment, which was (the same as in Skákala et al. (2020)) forced by an external product extrapolated from the 443 nm data of Smyth and Artioli (2010). The bio-optical module was extensively validated in Skákala et al. (2020), and was shown to be skilled in its representation of SWR, PAR and the underwater irradiances.

Table 1
The different light schemes forcing the heat fluxes in the physical NEMO model. The abbreviations can be explained as follows: (1) "Chl *a*": chlorophyll *a*, (2) "ady": ERSEM tracer representing absorption by particulate organic matter (POM), coloured dissolved organic matter (CDOM) and sediment.

Abbreviation	Two-way coupling	Source of incoming SWR	Resolved	Attenuation scheme	The studies using this scheme
NO-BGC	No	Bio-optical module	33 bands, diffuse, direct	OASIM only clear water	–
1-WAY	No	ERA5	Visible, invisible (2 bands)	Visible: 490 nm K_d product, invisible: clear water	(Skákala et al., 2018, 2020, 2021)
1-WAY-RGB-CC	No	ERA5	Visible: 3-bands (RGB), invisible: 1-band	Visible: 0.05mg/m^3 Chl *a*, visible, invisible: clear water	(Lengaigne et al., 2007; O'Dea et al., 2017; Graham et al., 2018)
2-WAY-RGB-SC	Yes	ERA5	Visible: 3-bands (RGB), invisible: 1-band	Visible: ERSEM Chl *a*, visible, invisible: clear water	(Lengaigne et al., 2007)
2-WAY	Yes	Bio-optical module	33 bands, diffuse, direct	OASIM, ERSEM 4 PFT Chl *a*, forced ady, clear water	–

Finally, all the ERSEM simulations in this study used the bio-optical module described in the previous paragraph, but in the case of the NO-BGC run (for abbreviations see Table 1) all the attenuation except by the clear sea water was removed. The choice of ERSEM light scheme for the different simulations is justified as follows:

(a) The 1-WAY and 2-WAY configurations using the bio-optical module to force ERSEM, correspond to the latest research version of the CMEMS system on the NWES (the 1-WAY configuration, see Skákala et al. (2020)) and the currently most advanced version of the coupled NEMO-FABM-ERSEM model on the NWES (the 2-WAY configuration).

(b) To sensibly compare the impact of biogeochemistry on physics it is important that the 2-WAY-RGB-SC run (Table 1) uses the same ERSEM light module as the 2-WAY run. This ensures that the simulated biogeochemical tracers are between the different two-way coupled runs consistent to a maximum possible degree, in the sense that the only differences in the ERSEM tracers are caused by the differences in the NEMO physics (transport, mixing, temperature), triggered by the different NEMO light schemes.

(c) In case of both, NO-BGC and 1-WAY-RGB-CC runs, NEMO is entirely independent from ERSEM. It is also expected that the physics in the NO-BGC and 1-WAY-RGB-CC will be the most different from the remaining three free simulations. To estimate the size of the impact of the NEMO simulated physical state on the ERSEM simulated biogeochemistry, relative to the size of the impact of the radiances seen by ERSEM, whilst minimizing the number of necessary simulations included in the study, we decided to use the same ERSEM light scheme for the 1-WAY-RGB-CC run as for the 1-WAY, 2-WAY and 2-WAY-RGB-SC runs, but using the same light scheme for ERSEM as in NEMO for the NO-BGC run.

2.3. The assimilative system: NEMOVAR

NEMOVAR is a variational (in this study a 3DVar) DA system (Mogensen et al., 2009, 2012; Waters et al., 2015) used at the Met Office for operational forecasting and reanalyses on the NWE Shelf. The assimilation of ocean colour-derived chlorophyll using NEMOVAR is highly successful in improving the NWE Shelf phytoplankton phenology, PFT community structure (using PFT chlorophyll assimilation), underwater irradiance and to a more limited degree also carbon cycle (Skákala et al., 2018, 2020; Kay et al., 2019). NEMOVAR includes capability to assimilate multi-platform (satellite, in situ) data, which has been established first for physics (e.g. Waters et al. (2015), King et al. (2018)) and subsequently for biogeochemistry (Ford, 2021), including validating the multi-platform DA system for the NWES (Skákala et al., 2021).

The NEMOVAR set-up used in this study for the multi-platform physical–biogeochemical assimilation is the same as the one described in detail by Skákala et al. (2021). Here we offer only a short summary: The 3DVar version of NEMOVAR uses a First Guess at Appropriate Time (FGAT) to calculate a daily set of increments for the directly updated variables (Waters et al., 2015; King et al., 2018). In the physical DA application, NEMOVAR applies balancing relationships within the assimilation step and delivers a set of increments for temperature, salinity, sea surface height (SSH) and the horizontal velocity components. For the total chlorophyll assimilation NEMOVAR calculates a set of log-chlorophyll increments and then a balancing scheme is used to distribute those increments into the PFT components (chlorophyll, carbon, nitrogen, phosphorus and for diatoms also silicon), all of which are updated based on the background community structure and stoichiometric ratios (e.g. Skákala et al. (2018, 2020, 2021)). After the assimilation step, the model is re-run with the increments applied to the model variables gradually at each model time-step using incremental analysis updates (IAU, Bloom et al. (1996)).

NEMOVAR uses externally supplied spatio-temporally varying observation and background error variances, with the background error variances typically 1–3 times larger than the observational error variances (Skákala et al., 2021). The system combines two horizontal correlation length-scales, one fixed at 100 km and the other based on the baroclinic Rossby radius of deformation (King et al., 2018). The vertical length-scales follow the scheme from King et al. (2018), where NEMOVAR calculates directly the set of 3D increments using flow-dependent vertical length-scales (ℓ), which are at the surface equal to half of the MLD, decreasing in the mixed layer to become two-times the vertical model grid spacing at, and beneath the MLD.

2.4. Observations: assimilated and validation data

2.4.1. Assimilated data

In the physical data assimilation component we have included:

(a) sea surface temperature data from the GCOM-W1/AMSR-2, NOAA/AVHRR, MetOp/AVHRR, MSG/SEVIRI, Sentinel-3/SLSTR, Suomi-NPP/VIIRS satellite products and in situ SST observations from ships, surface drifters and moorings, distributed over the Global Telecommunication System (GTS) in near-real time,

(b) temperature and salinity from the EN4 dataset (Good et al., 2013), which includes in situ profiles from Argo floats, fixed moored arrays, XBTs, CTDs, gliders, marine mammals, and

Table 2
The AlterEco gliders and the variables measured by the gliders used for assimilation (6-th column), or validation (7-th column). The table uses the following abbreviations: deployment:"dpl", data assimilation:"DA", temperature:"T", salinity:"S", oxygen concentrations:"O_2", chlorophyll *a* concentrations:"Chl *a*" and sum of nitrate and nitrite concentrations:"NO_x^-".

Campaign	Platform	dpl	Serial	Mission period	DA	Validation
AlterEco 1	Stella	440	unit_436	02/02/2018 - 08/05/2018	none	T,S,O_2,Chl *a*
AlterEco 1	Cook	441	unit_194	15/11/2017 - 07/02/2018	none	T,S,O_2,Chl *a*,NO_x^-
AlterEco 2	Orca	493	SG510	07/03/2018 - 27/03/2018	none	Chl *a*,NO_x^-
AlterEco 2	Melonhead	496	SG620	07/02/2018 - 02/04/2018	none	Chl *a*
AlterEco 3	Cabot	454	unit_345	08/05/2018 - 15/08/2018	T,S,Chl *a*	T,S,O_2,Chl *a*
AlterEco 3	Orca	455	SG510	16/03/2018 - 24/07/2018	none	Chl *a*,NO_x^-
AlterEco 3	Humpback	497	SG579	09/05/2018 - 25/06/2018	none	Chl *a*
AlterEco 4	Dolomite	477	unit_305	13/08/2018 - 10/10/2018	none	T,S,Chl *a*,NO_x^-
AlterEco 4	Eltanin	478	SG550	15/08/2018 - 28/09/2018	none	Chl *a*
Altereco 5	Kelvin	481	unit_444	26/09/2018 - 02/12/2018	none	T,S,Chl *a*
AlterEco 6	Dolomite	499	unit_305	02/12/2018 - 12/03/2018	none	T,S,O_2,Chl *a*
AlterEco 6	Coprolite	500	unit_331	02/12/2018 - 12/03/2018	none	T,S,O_2,Chl *a*

(c) temperature and salinity data from a specific Slocum glider Cabot (Unit 345, see Skákala et al. (2021)) that was deployed in the central North Sea during 08/05/2018 - 15/08/2018 as a part of the Alternative Framework to Assess Marine Ecosystem Functioning in Shelf Seas (AlterECO) programme (https://altereco.ac.uk/). The satellite SST was bias-corrected following the scheme from While and Martin (2019), using the VIIRS and in situ SST data as the reference.

In the biogeochemical data assimilation we have included total log-chlorophyll derived from the version 4.2 of the European Space Agency (ESA) ocean-colour (OC) Climate Change Initiative (CCI) product (Sathyendranath et al., 2019) and also log-chlorophyll derived from the quenching corrected fluorescence measurements by the same AlterEco glider Cabot, that was used in the physical data assimilation. The assimilation is performed for log-chlorophyll, rather than chlorophyll, as chlorophyll is widely known to be log-normally distributed (Campbell, 1995).

The assimilated in situ (EN4 and glider) observations were thinned to a resolution of 0.08° (EN4), or up-scaled to the AMM7 grid (glider), with additional temporal averaging applied to the same-day glider observations. The thinning/up-scaling is performed to avoid assimilating many observations at higher resolution than the model can represent. After the thinning/up-scaling there were O(10^5) EN4 and O(10^4) Cabot glider data-points to assimilate throughout the year 2018.

2.4.2. Validation data

The assimilated data, mentioned in the previous section, were also used to validate every experiment where they were excluded from the assimilation (e.g. assimilated chlorophyll data were used to validate free runs and the physical data assimilative runs). However, we excluded the bias-corrected satellite SST from the temperature validation, so that the only assimilated SST data used for validation were a) the high quality SST data from the VIIRS satellite product and from ships, drifters and moorings (we will call this "VIIRS/in situ SST data"), and the SST that was part of b) EN4 and c) Cabot glider data.

Besides the assimilated observations, all the experiments were validated with other (non-assimilated) AlterEco glider data for temperature, salinity, chlorophyll, oxygen and the sum of nitrate and nitrite (all the gliders included in the validation are listed in Table 2). The processing of the physical, chlorophyll and oxygen data was described in Skákala et al. (2021). The sum of nitrate and nitrite concentrations (abbreviated as $NO_x^- = NO_3^- + NO_2^-$) were determined using a Lab-on-Chip (LoC) analyser designed and fabricated at the National Oceanography Centre (Beaton et al., 2012), which was implemented by the AlterEco team into Seagliders following a similar protocol as used by Vincent et al. (2018). The combined uncertainty (random and systematic errors) of measurements made using these LoC analysers has been calculated as <5% (coverage interval $k = 1$) (Birchill et al., 2019). The nitrite concentrations were relatively negligible compared to the nitrate concentrations, so the NO_x^- data were used to validate model nitrate outputs. All the data used here is from AlterEco gliders that were in operation in the central North Sea during 2018 (for both the glider and the EN4 data locations see Fig.S1 of the Supporting Information (SI)), moving throughout the whole water column. Similar to the assimilated Cabot glider, the remaining glider data were up-scaled onto the model grid (on a daily basis) and after the up-scaling there remained O(10^4) AlterEco glider observations for each variable in 2018.

The EN4 data-set contained subsurface observations that were approximately homogeneously distributed both with depth and in time, with a slightly lower number of observations towards the end of the year (November–December 2018). Beyond the assimilated data and the AlterEco data, we used for validation a 1960–2014 monthly climatological dataset for total chlorophyll, oxygen, nitrate, phosphate and silicate concentrations, compiled during the North Sea Biogeochemical Climatology (NSBC) project (Hinrichs et al., 2017). The NSBC dataset covers most of the NWE Shelf and the full range of depths. Finally, we also included validation of surface CO_2 fugacity using 2018 SOCAT (v2019) data (https://www.socat.info/index.php/about/).

2.5. The experiments

As outlined in Table 1 we have run multiple free simulations including both one-way coupled and two-way coupled runs. We also tested the impact of assimilating different types of data (physical-only, biogeochemical-only and physical and biogeochemical jointly, see Table 3) on the skill of both 1-WAY and the 2-WAY models. The various free and assimilative experiments used exactly the same model configuration, apart from the differences outlined in Tables 1 and 3. The experiments all started from the same initial value conditions on the 01/09/2017 to allow a 4 month spin-up time for the final 2018 simulation. The initial values were provided by the 2016–2018 free simulation (using bio-optical module) from the study of Skákala et al. (2020).

2.6. Skill metrics

The performance of the different simulations is evaluated using two skill metrics. The first metric is the model bias (ΔQ_{mo}):

$$\Delta Q_{mo} = \langle Q_m - Q_o \rangle \tag{2}$$

where Q_o are the observations mapped into the model grid and the Q_m are the corresponding model outputs. The second metric is the bias-corrected root mean square difference (BC RMSD, $\Delta_{RD} Q_{mo}$):

$$\Delta_{RD} Q_{mo} = \sqrt{\langle (Q_m - Q_o - \Delta Q_{mo})^2 \rangle}. \tag{3}$$

Table 3
The different assimilative experiments compared in this study. The first column shows the abbreviated experiment name, where the last word in the name ("1-WAY", "2-WAY") refers to the baseline model configuration (see the third and sixth rows of Table 1) and the following columns list the assimilated data. The table uses the following abbreviations: satellite:"sat", Cabot glider:"Cabot", EN4 dataset:"EN4", temperature:"T", sea surface temperature:"SST", salinity:"S", chlorophyll *a*:"Chl *a*".

Abbreviation	SST (sat./in situ)	T & S (EN4)	T & S (Cabot)	Chl *a* (sat.)	Chl *a* (Cabot)
PHYS DA 1-WAY	yes	yes	yes	no	no
PHYS DA 2-WAY	yes	yes	yes	no	no
CHL DA 1-WAY	no	no	no	yes	yes
CHL DA 2-WAY	no	no	no	yes	yes
PHYS+CHL DA 1-WAY	yes	yes	yes	yes	yes
PHYS+CHL DA 2-WAY	yes	yes	yes	yes	yes

3. Results

3.1. The impact of biogeochemistry on physics on the NWES

To determine the overall impact of biogeochemical light attenuation on the NWES temperature vertical profiles, we compare the simulation based on the bio-optical module using only clear water attenuation (NO-BGC) with the two-way coupled run using the bio-optical module and assimilating chlorophyll into the model (CHL DA 2-WAY). The CHL DA 2-WAY run is chosen because it provides us with the best representation of the biogeochemical feedback to physics including the most realistic simulation of the phytoplankton distributions.

Fig. 2 shows that NWES biogeochemistry has a substantial impact on the simulated temperature in the late spring–summer, heating up the upper 20 m in the water column and cooling down the water column beneath the mixed layer, almost down to the 200 m depth. The temperature variations due to biogeochemistry are, in the warmest summer period, on the scale of ± 1°C. The geographical impact of biogeochemistry on temperature (Fig. 3:A) is largest in the northern part of the North Sea. Conversely, it is by far the lowest in the English Channel and the southern part of the North Sea. The heating of the uppermost ocean layer has an important impact (up to 20%) on the mixing depth, which is consistently shallowed by the biogeochemistry across the whole NWES (Fig. 3:C).

All the results presented in this section are broadly consistent with the findings of Manizza et al. (2005) for the global domain and Oschlies (2004) more specifically for the North Atlantic domain.

3.2. Comparing the impact of different light schemes on physics

We compare the sensitivity of simulated temperature and MLD to the light schemes, incorporating the impact of biogeochemistry on the light attenuation seen by the NEMO physical model (Table 1). Figs. 4 and 5 compare the temperature of all the simulations using different light schemes to the NO-BGC run. Fig. 4 shows that the two-way coupled model based on the bio-optical module (2-WAY, panel D) produces an increase of near-surface attenuation, and hence sea temperature, when compared to the one-way coupled run forced by an external satellite product (1-WAY, panel B, for direct comparison between the two runs see also Fig.S2 of the Supporting Information, SI).

Since the physical model skill depends on many components within the complex model, there can be many error compensations (Skákala et al., 2020). It is, therefore, hard to validate the performance of the NEMO light scheme independently of the specific context in which it was implemented. However, Fig. 5 should still give an indication of how the different light schemes compare with the 3D glider observations along the glider trajectory. Fig. 5 illustrates that neglecting the biogeochemical impact on light attenuation in the NO-BGC run produces a spurious heating effect of up to 3 °C beneath the upper 30 m in the water column. Including biogeochemical impact on the temperature reduces this model bias to below 1 °C (Fig. 5:B–E).

3.3. The sensitivity of biogeochemistry to the changes in underwater radiance and mixing

ERSEM is known to simulate a late phytoplankton spring bloom on the NWES (e.g. Figs. 6 and 7). As suggested by the critical turbulence hypothesis, the bloom timing depends on both, the light seen by the phytoplankton, and vertical mixing (e.g. Fig. 1). The ERSEM sensitivity to light is demonstrated by the NO-BGC simulation. Due to absence of biogeochemical impact on the underwater radiances in the NO-BGC run, there is an excess of light deep within the water column and this provides (despite the deep winter mixing) good phytoplankton growth conditions over the winter, with an early bloom triggered around late February (Fig. 6:B). The only seriously limiting factor to the surface chlorophyll abundance in the NO-BGC run seem to be nutrients in the post-bloom period (Fig. 6:B).

In the remaining free run simulations, ERSEM always uses the same light scheme, but the physical NEMO model does not. The different light schemes in the physical model produce different vertical mixing and slightly modify the timing of the phytoplankton bloom (Fig. 6:C–D). For example, the increased near-surface absorption in the 2-WAY model increases heating in the upper oceanic layer with respect to the 1-WAY run (Fig. 4:B,D), reduces convective mixing, and for most of the NWES, moves the model bloom towards the start of the year by 1–3 days, but in some specific locations (e.g. in the central North Sea) the bloom can be as much as 5 days earlier in the 2-WAY run than in the 1-WAY run (Fig. 6:C,E, Fig. 7:C, Fig. 8).

3.4. The potential impact of two-way coupling on the skill of the CMEMS operational system

Introducing two-way coupling into the CMEMS operational model would correspond to a transition from the 1-WAY to the 2-WAY model set-up, but also include the assimilation of physical and biogeochemical data. As previously discussed in the free run, the transition from 1-WAY to 2-WAY run produces extra heating in the upper 20 m of the ocean, increasing sea temperature by around 1 °C, and by a similar margin cooling down the 20–100 m layer beneath the surface (compare Fig. 4:A and Fig. 4:D, Fig.S2:B of the SI). This marginally shallows the MLD (Fig. 4:E).

In the summer (May–October), when the impact of two-way coupling is largest, the 2-WAY run reduces the temperature bias of the 1-WAY run, however it increases the SST bias and BC RMSD (Fig. 9:A). In the winter (November–April), the impact of two-way coupling on the model temperature is also mixed (Fig. 9:B), as it is for salinity throughout the whole year (Fig. 9:C–D). The changes to physics introduced by the 2-WAY set-up (relative to 1-WAY) have a positive impact on the timing of the phytoplankton bloom (Fig. 6:C,E, Fig. 7:C), which leads to improvement in model skill in representing phytoplankton chlorophyll *a* (Fig. 10:A). Interestingly, correcting phytoplankton phenology through the OC chlorophyll assimilation has also a positive impact on the simulated temperature and salinity in the 2-WAY run (Fig. 9). Fig. 9 also demonstrates that the physical (temperature and salinity) assimilation substantially improves model skill in representing both

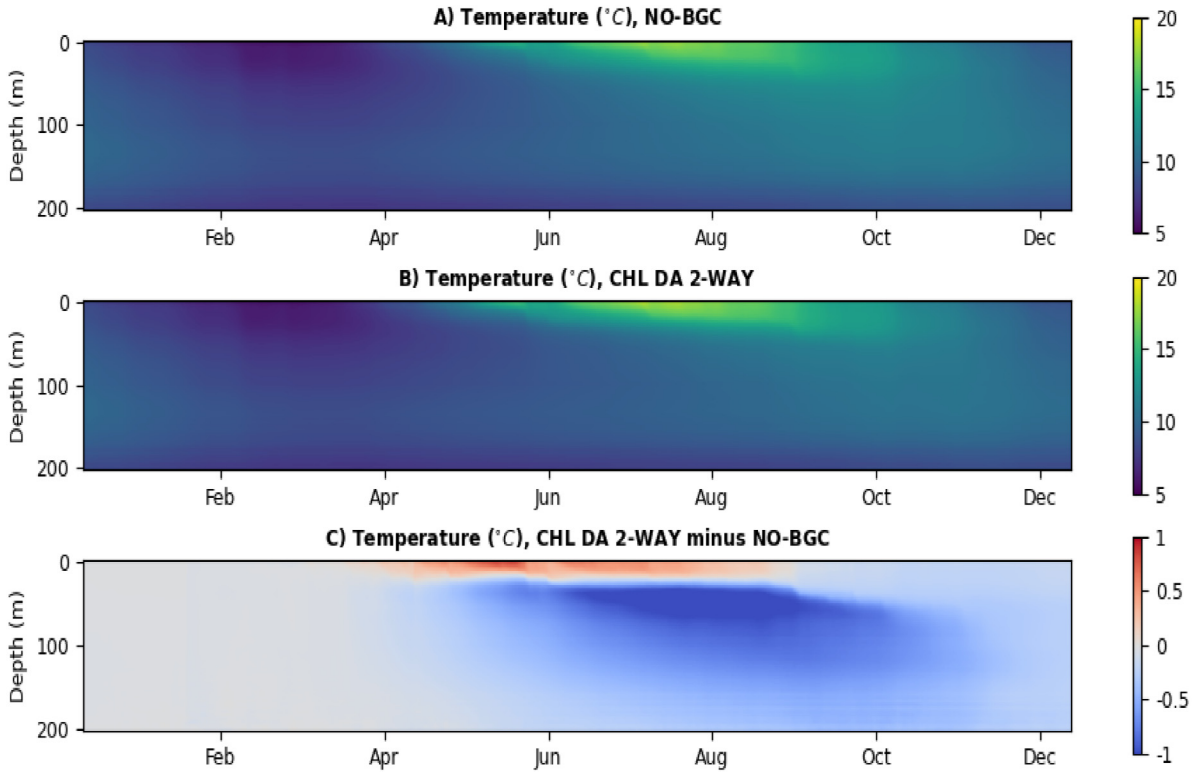

Fig. 2. Panel A shows a Hovmöller diagram (depth on the *y*-axis vs time on the x-axis) for the temperature (°C) of the run with only sea water attenuation. The values for each day and depth represent the horizontal spatial averages throughout the NWES (bathymetry < 200 m, see the boundary in Fig. 3). Panel B shows the same Hovmöller diagram as panel A, but for the CHL DA 2-WAY run (for the abbreviations used in the titles see Table 3), whereas panel C shows the difference between the two runs shown in the panels A and B (panel B minus panel A).

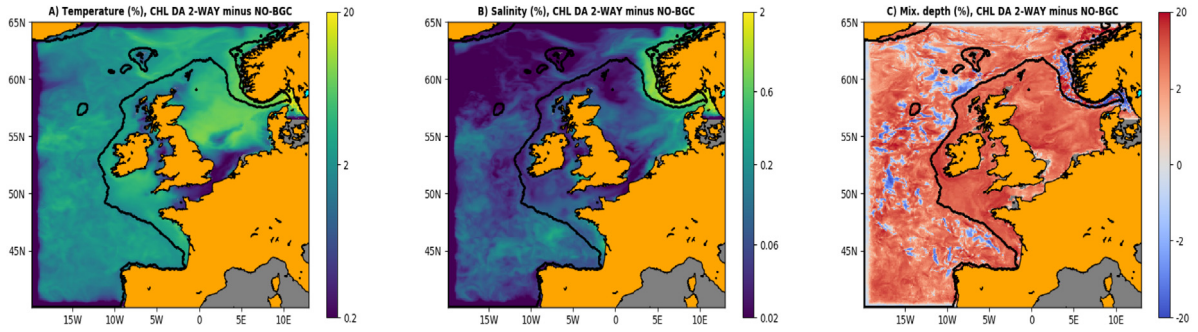

Fig. 3. The spatial regions of biogeochemical impact on temperature (A, in %), salinity (B, in %) and mixing depth (C, in %). For temperature and salinity the panels show 2018 and vertically (up to 200 m depth) averaged absolute difference between the CHL DA 2-WAY and NO-BGC runs normalized by the values of the NO-BGC run (in case of temperature, the normalization is relative to Celsius). For mixing depth (defined as the maximum depth of the column where the temperature difference between top and bottom layer is less than 0.2 °C) we show the mean 2018 difference between CHL DA 2-WAY and NO-BGC runs normalized by the NO-BGC run. The boundary of the NWES (bathymetry < 200 m) is marked by the black line.

temperature (Fig. 9:A–B) and salinity (Fig. 9:C–D). The physical data assimilation influences the simulated temperature more evenly across the water column than the bio-optical module (Fig.S2 of SI), which is likely a combination of model dynamical response to the temperature increments in the mixed layer and some assimilated sub-surface data (EN4 and Cabot glider).

The chlorophyll assimilation improves the simulated chlorophyll (Fig. 10:A), and dominates over both physical assimilation and two-way coupling in its impact on the simulated chlorophyll concentrations across the whole water column over the whole simulation year (Fig.S3 of SI). That this would be the case is not obvious, as the chlorophyll assimilation is almost entirely based on the satellite OC and chlorophyll beneath the mixed layer is updated mostly through the model dynamical adjustment. The bloom dynamics is also corrected by the chlorophyll assimilation (Fig.S4 of SI), which is consistent with the previous studies (Skákala et al., 2020, 2021).

To get a more complete view of the impact of two-way coupling on the simulated biogeochemistry, we also looked at the available data for oxygen, CO_2 fugacity, nitrate, phosphate and silicate. Fig. 10 shows that the two-way coupling may also improve the modelled oxygen (Fig. 10:B) and CO_2 fugacity (Fig. 10:C), which is, in both cases, a combined result of changes to air–sea fluxes (due to changes in sea temperature and therefore gas saturation levels), to the primary productivity (change to bloom timing) and consequently also changes to respiration levels. Physical and chlorophyll *a* assimilation tend to have additional positive impact on oxygen and CO_2 fugacity (Fig. 10:B–C). The impact of the two-way coupled model on nutrients is mostly driven by the changes to primary productivity and phytoplankton, and is shown to be fairly negligible (Fig. 10:C–F). These results are broadly

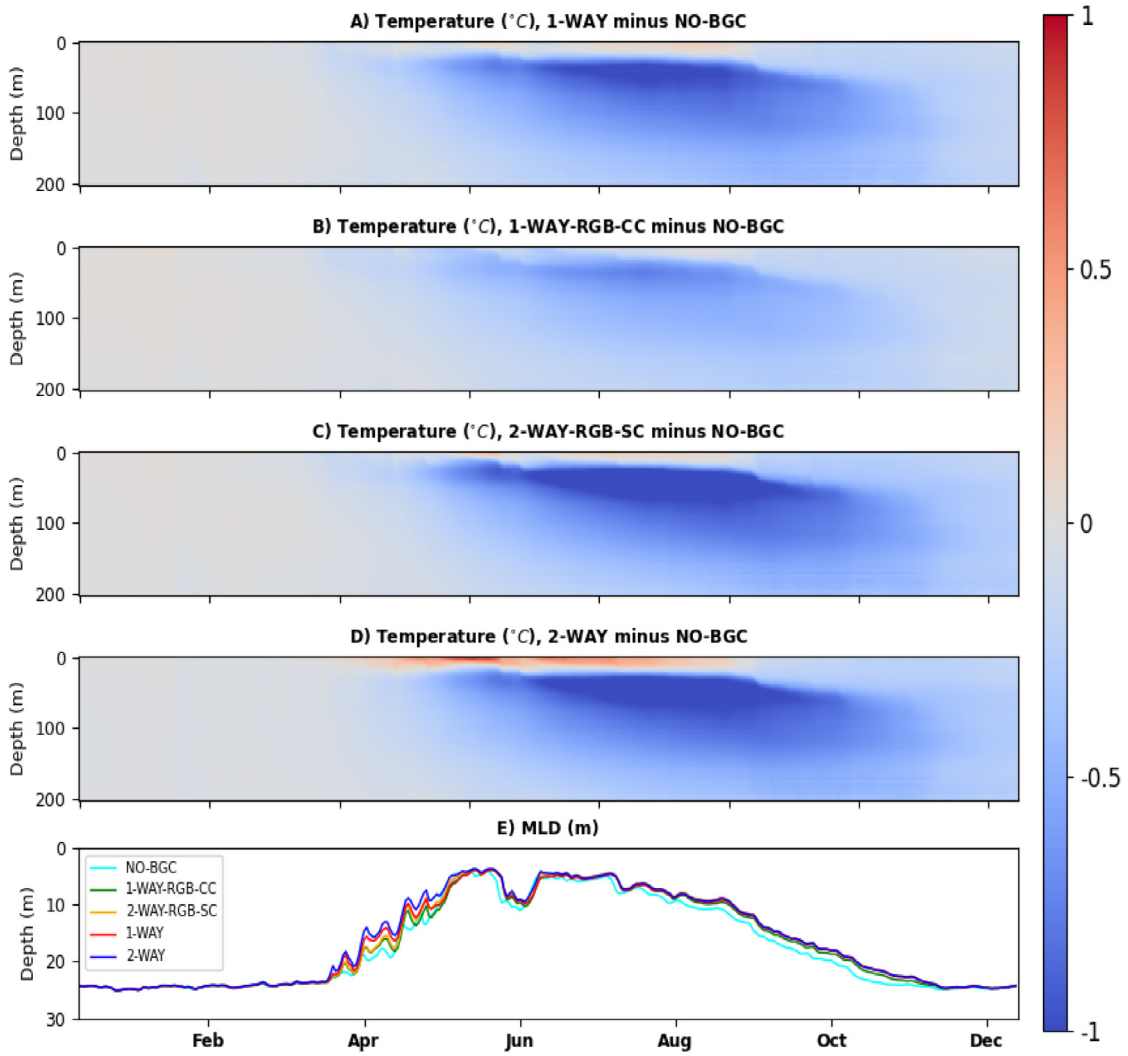

Fig. 4. Panels A–D are similar to Fig. 2:C and show Hovmöller diagrams for the horizontally averaged differences in temperature (in °C, averaged across NWES) between the different light schemes and the NO-BGC run. Panel E compares the 2018 time series for MLD (in m) horizontally averaged across the NWES.

consistent with the previous literature (Skákala et al., 2018, 2020), which showed that chlorophyll *a* assimilation can have an important impact on the nutrient concentrations, but often has a mixed effect in terms of the model skill to represent nutrients (Fig. 10).

4. Discussion

On the NWES, there is a strong seasonal dependence of the biogeochemical impact on temperature (Fig. 2) which can be easily understood: in the late autumn to early spring period the water column is very well mixed and this averages out the vertical changes to heating caused by the presence of biogeochemical tracers. In the late spring, when the water column becomes much more stratified, the biogeochemical substances trap light and heat in the uppermost layer, gradually cooling down the ocean beneath the upper ~ 20 m. However, due to oceanic inertia, the impact of extra near-surface heating introduced by the biogeochemical substances propagates only slowly downwards, producing an increasingly delayed response (approximately on a monthly scale) as one looks deeper into the water column (Fig. 2:C). Similarly to the winter period, the lack of biogeochemical impact on physics around the English Channel (Fig. 3) can be explained by the high levels of vertical mixing in this area (see O'Dea et al. (2012)).

The 2-WAY run produces large extra heating in the uppermost layer also relative to the 1-WAY run (Fig. 4:A,D). Although, in theory, the bio-optical module used to drive biogeochemistry produces different incoming radiation than the ERA5 forcing data used to force physics in the 1-WAY run, it has been shown that there is a negligible mutual bias between the module and ERA5 (Skákala et al., 2020). Therefore, the temperature increase is likely a consequence of an increased rate of absorption inside the upper oceanic layer, rather than resulting from an enhanced shortwave radiation flux into the water column. The increased absorption in the 2-WAY run was anticipated since: a) in a previous study (Skákala et al., 2020) the bio-optical module appeared to have higher levels of light attenuation near the water surface than the satellite observations used to force the physics in the one-way coupled run, b) the "broadband" visible light attenuation in the 1-WAY run was represented by the satellite K_d for 490 nm wavelength, but K_d at 490 nm wavelength is clearly an underestimate of the K_d for the 400–700 nm waveband (see Fig. 5:B of Skákala et al. (2020)).

We can also understand the gradually increasing impact of biogeochemistry on temperature between the 1-WAY-RGB-CC, 2-WAY-RGB-SC and 2-WAY runs (Fig. 4:B–D). The RGB scheme using constant chlorophyll (1-WAY-RGB-CC, Fig. 4:B, used in Lengaigne et al. (2007), O'Dea et al. (2017), Graham et al. (2018)) to represent oligotrophic open ocean waters, clearly underestimates the overall chlorophyll concentrations in the shelf seas and leads to unrealistically small attenuation of underwater radiance. The attenuation is increased by the more realistic simulated chlorophyll in the 2-WAY-RGB-SC run (Fig. 4:C),

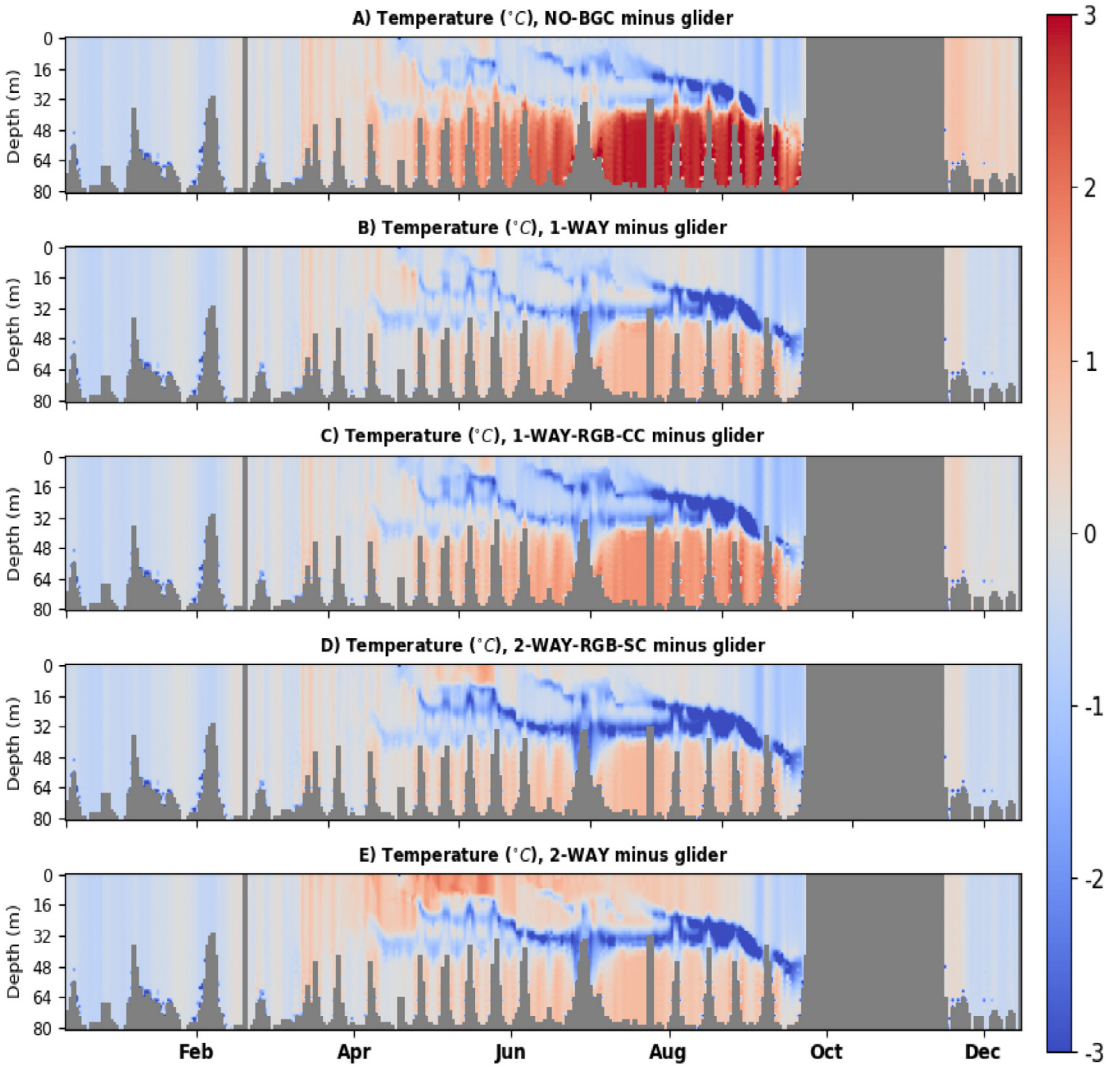

Fig. 5. Hovmöller diagrams comparing the temperature (in °C) in the different free runs to the glider data along the glider trajectory.

but it remains weak when compared to the 2-WAY scheme, since 2-WAY-RGB-SC neglects the impact of POM, CDOM and sediment on the light attenuation. These non-living optically active constituents can be potentially neglected in the open ocean (e.g Lengaigne et al., 2007)), but become more relevant in the coastal and shelf sea waters, as these results demonstrate. The 2-WAY scheme (Fig. 4:D) incorporates the impact of all phytoplankton, POM, CDOM and sediment on the underwater radiance, and therefore demonstrates the greatest impact of biogeochemistry on temperature. The sensitivity of physics to biogeochemical attenuation scheme, that we observed here, is also broadly consistent with an older modelling study of Baird et al. (2007), focusing on the seas near the south-eastern coast of Australia, which has found that the simulated temperature vertical profiles and some ocean circulation patterns were significantly impacted by the chlorophyll vertical attenuation scheme.

The shift in the bloom timing shown in Fig. 8 nicely matches with the regions where there is the largest biogeochemical impact on temperature (Fig. 3:A). This indicates that, although the bloom timing was shown not to be very sensitive to the changes in convective mixing (e.g. Fig. 6), the small changes to the bloom timing can be understood from the critical turbulence hypothesis (as outlined in Fig. 1). In reality the late bloom could be explained by multiple components within the physical–biogeochemical coupled model, such as atmospheric wind stress forcing, NEMO upper-ocean mixing scheme, vertical stratification (thermocline and pycnocline), incoming surface PAR, underwater light attenuation, the phytoplankton growth response to light (e.g. ERSEM parameters, such as P–I curves, or maximum PFT chlorophyll-to-carbon ratios), ERSEM representation of top-down grazing, or missing processes such as mixotrophy (e.g. Leles et al. (2018)). From the variety of drivers that could contribute to the bloom timing, only a small fraction was so far addressed, i.e. Skákala et al. (2020) have showed that the late bloom is most likely not related to a problem with the underwater radiances, whilst in this study we similarly addressed the vertical stratification. Diagnosing the true cause of the late phytoplankton bloom thus remains a challenge for the future.

Although the (modest) improvements to the simulated chlorophyll by the 2-WAY model originate from its changes to the simulated physics (i.e. vertical mixing), it might seem surprising that the physical data assimilation, which substantially improves the simulated physics (Fig. 9), does not improve (and even slightly degrades) the model skill in chlorophyll (Fig. 10:A). This is likely because the physical data assimilation is, for the large part, an assimilation of SST. The improvement in the ecosystem model skill depends mostly on the vertical mixing and limited changes to vertical mixing are expected by assimilating SST. Assimilated subsurface temperature and salinity data are quite sparse, and have only a limited impact on the modelled biogeochemistry. In the case of the Cabot glider "case-study", the glider temperature and salinity assimilation did not improve the simulated chlorophyll at the glider locations (Fig. 10:A) mostly because the impact of physics on biogeochemistry needs some spin-up time. In fact in the last part of

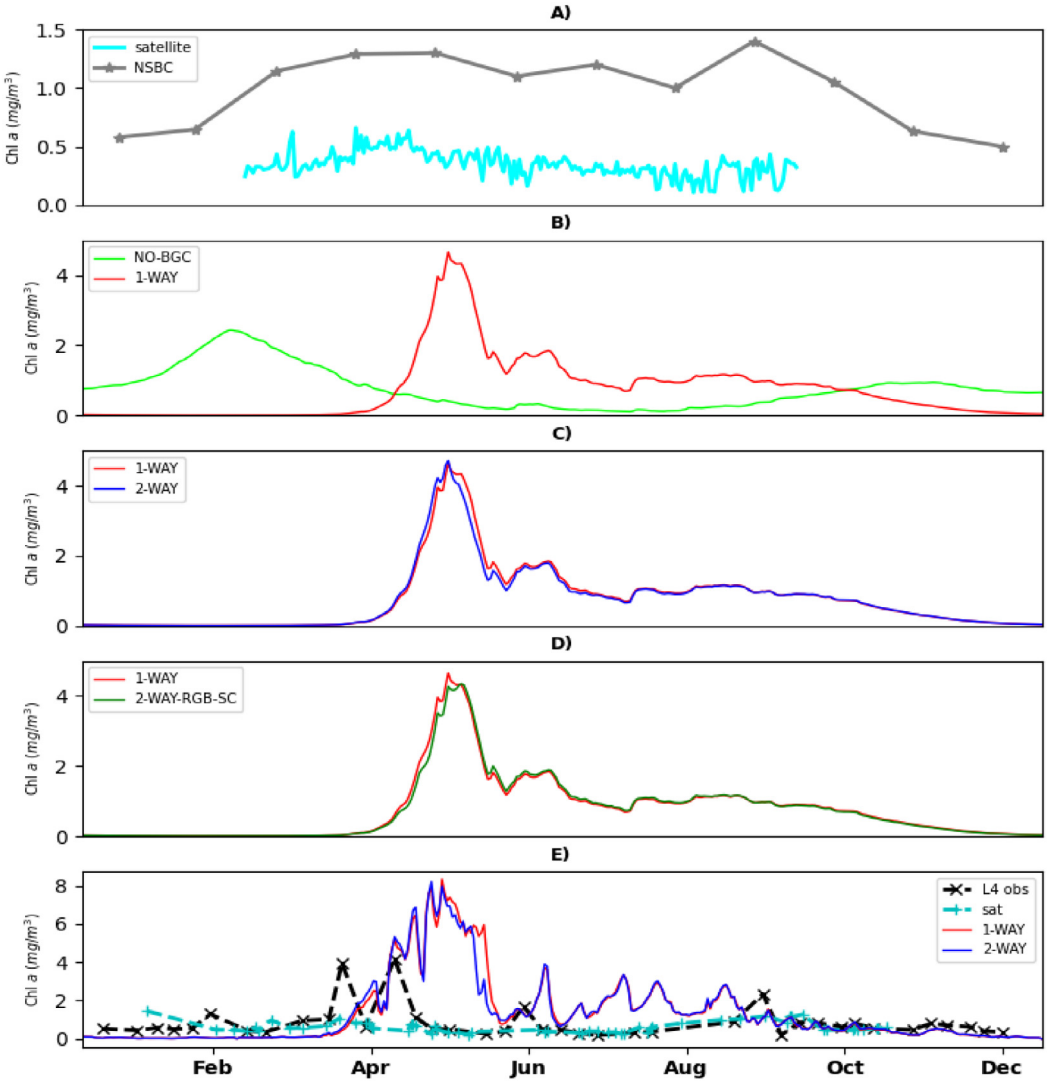

Fig. 6. Panels A–D show the 2018 time-series for the surface chlorophyll (mg/m^3) averaged across the NWES. Panel A is showing the satellite OC observations and NSBC climatology, whilst panels B–D compare the selected light schemes. The last panel E compares the model, satellite and in situ observations at the L4 station in the English Channel.

the glider mission period (late July–August) the physical assimilation has some potential to improve the chlorophyll concentrations, as was demonstrated by the assimilation of the same Cabot glider data in Fig. 6E of Skákala et al. (2021).

There is only negligible difference in the skill between the PHYS+CHL DA 1-WAY and PHYS+CHL DA 2-WAY runs (Figs. 9 and 10). This suggests that physical and chlorophyll assimilation dominates over the two-way coupling and hence, for an operational system that includes assimilation of both physics and biogeochemistry, the transition to two-way coupling may produce only marginal difference in the system skill. Such difference might certainly be more significant for system forecasts than for the analyses (forecasting was not explored in this study). However, on the 1-day time scale the forecast differences were captured by the difference in innovations (defined as background minus observations) and this was found to be negligible, e.g. the 2018 and spatial mean difference in the SST innovations between the PHYS+CHL DA 1-WAY and PHYS+CHL DA 2-WAY runs was found to be less than 0.01 °C.

5. Summary

In this work we used a recent implementation of an (OASIM-based) spectrally resolved bio-optical module into a physical–biogeochemical model of the North-West European Shelf (NWES, Skákala et al. (2020)) and expanded it to drive also the oceanic heat fluxes, introducing a feedback from the biogeochemical model to the physics (we call the models with such feedback "two-way coupled models"). We used this development to estimate the scale of the biogeochemical impact on physics on the NWES and we have shown that during late spring and summer, when the water column is stratified, biogeochemical tracers can heat up the upper 20 m of the water column by 1 °C and cool down the ocean beneath the upper 20 m by a similar margin. The seasonal impact of biogeochemistry on physics propagates deeper into the water column with oceanic inertia and is visible down to 200 m depth. Impact of biogeochemistry on heating of the uppermost oceanic layer influences ocean vertical mixing and shallows the mixing depth across the NWES by up to 20%. These results suggest that it is important to represent the coupling from biogeochemistry to physics adequately in our models.

We have looked at different light schemes used in the literature (e.g. Lengaigne et al. (2007), O'Dea et al. (2017), Graham et al. (2018), Skákala et al. (2018)) that incorporate biogeochemical impact on light attenuation, either within a two-way coupled model, or as an external parametrization, or forcing (e.g. using 490 nm K_d satellite product). We have shown that the simulated physics is reasonably sensitive to the different light schemes, i.e. both to spectral resolution and the number of represented bio-optical tracers.

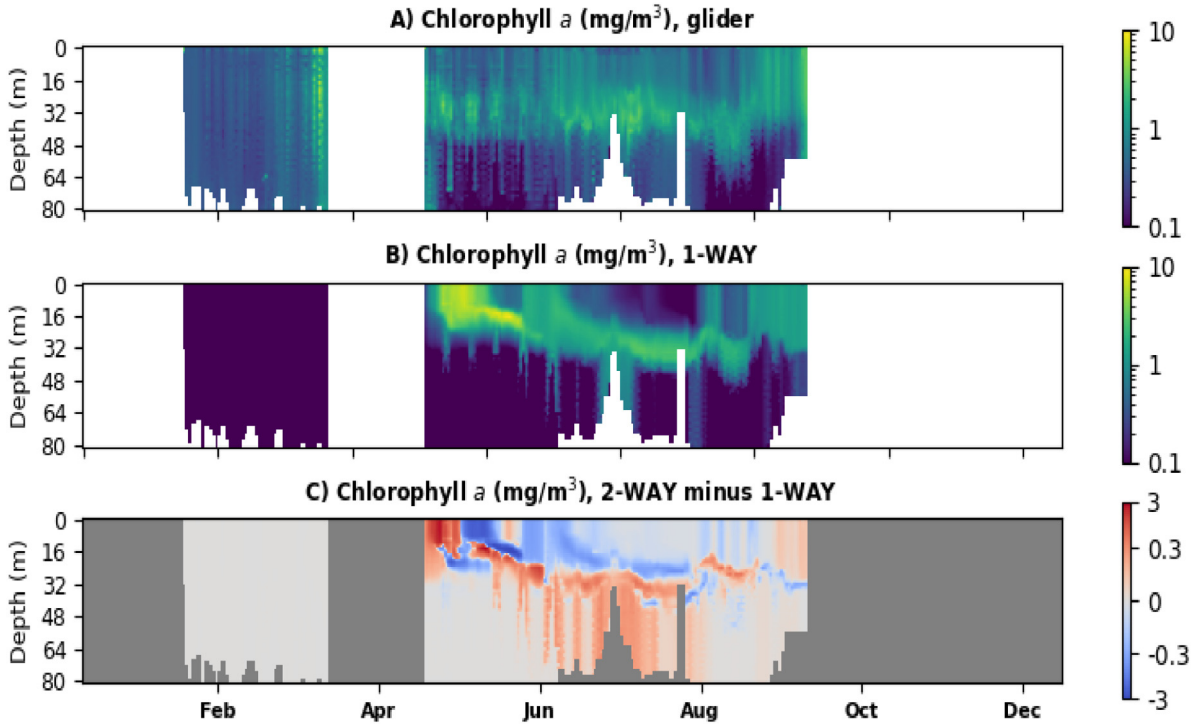

Fig. 7. Panels A–B show Hovmöller diagrams for chlorophyll (mg/m^3) observed by the AlterEco gliders (A) and simulated in the 1-WAY run across the glider trajectory (B). Panel C compares the 2-WAY and 1-WAY runs across the glider trajectory.

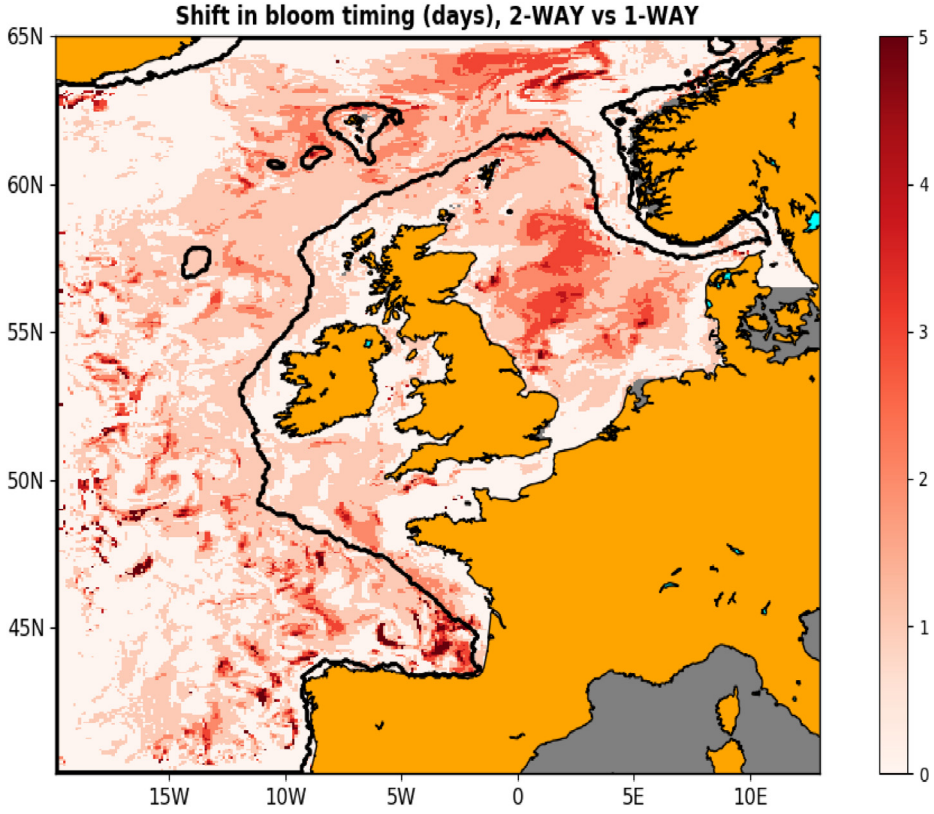

Fig. 8. The spatial distribution for the time-lag (in days) between the earlier bloom of the 2-WAY run and the later bloom of the 1-WAY run. The time-shift in the bloom was calculated by taking for each location the April–June total chlorophyll *a* time-series from both 1-WAY, 2-WAY, runs, extracting only the data when at least one of the runs had chlorophyll concentrations over 2 mg/m^3 threshold, and calculating from those data the time-lag with the highest lagged Pearson correlation between the two time-series.

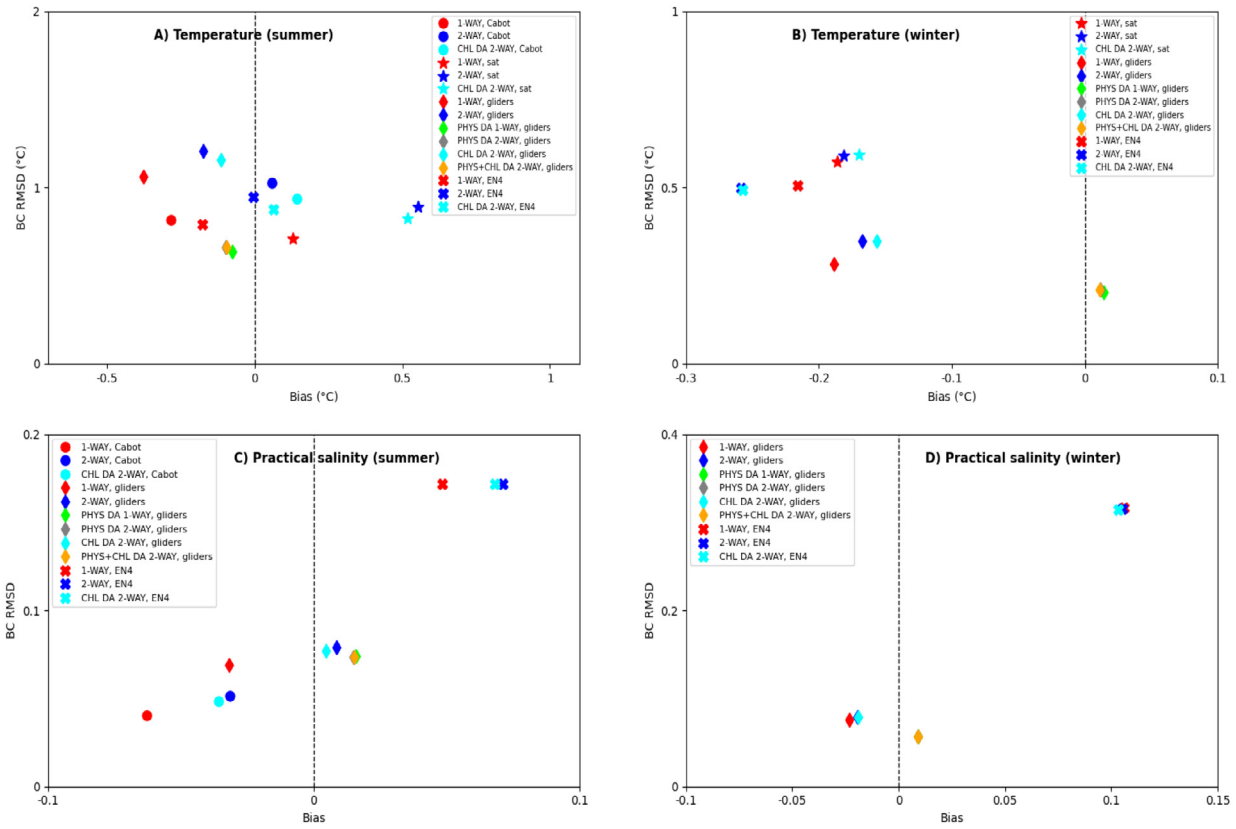

Fig. 9. Skill of the different model simulations to represent temperature (°C, panels A–B) and practical salinity (panels C–D). The skill is measured by bias (x-axis, Eq. (2)) and BC RMSD (y-axis, Eq. (3)). The skill is evaluated for two half-year periods of 2018, the "summer" (panels A,C) defined as May–October and the "winter" (panels B,D) defined as November–April (data averaged through January–April 2018 and November–December 2018). The different simulations are represented by different colours: 1-WAY (red), 2-WAY (blue), CHL DA 2-WAY (cyan), PHYS DA 1-WAY (lime), PHYS DA 2-WAY (grey) and PHYS+CHL DA 2-WAY (orange). The different markers show comparison with different data-sets: the star stands for the VIIRS/in situ SST, the circle for the Cabot glider observations, the diamond for the remaining available glider observations (the 2018 AlterEco mission without Cabot) and the cross for the EN4 data-set. The data (SST, Cabot, EN4) which were assimilated in some of the simulations were used to validate only the simulations that avoided their assimilation.

In the last part of this study we discussed the likely impact of introducing two-way coupling into the present operational CMEMS system for the NWES. We have shown that the newly developed two-way coupled model, based on the spectrally resolved bio-optical module, increases the heat captured in the upper part of the water column relative to the existing system, which represents the underwater attenuation by an external 490 nm K_d satellite product. The two-way coupling steepens the vertical temperature gradient, shallows the mixed layer depth and reduces convective mixing. The reduced vertical mixing has a modest, but positive, impact on the timing of the late bloom displayed by the biogeochemical model (in line with the critical turbulence hypothesis). The shift in the timing of the bloom in the two-way coupled model improves the model skill in representing chlorophyll. We conclude that, for a more substantial improvement of the timing of the bloom, it will be necessary to either improve the physical model mixing scheme, or to improve the process description, or parametrization, of the biogeochemical model. We have expanded our analysis to include other biogeochemical tracers, and found that the two-way coupled model and the physical data assimilation may sometimes help improve the agreement of simulated oxygen concentrations and CO_2 fugacity with observations, both due to improved simulation of the sea water temperature (saturation levels) and productivity.

Although the two-way coupled model performs slightly better than the existing one-way coupled model, it was found that the difference between those two becomes negligible whenever we include assimilation of physical data and chlorophyll. In the future it would be desirable to explore how much the impact of the two-way coupling increases during the 6-day operational forecasting period. Moreover, physical–biogeochemical assimilative runs on the NWES, including this work, are typically only weakly coupled (for one recent exception see Goodliff et al. (2019)), in the sense that the physical and the biogeochemical variables are updated independently and interact only through the model dynamics. The interaction between physics and biogeochemistry would be much more efficient if the assimilative updates to the physics and biogeochemistry interacted directly through their cross-covariances, or a balancing component within the data assimilation system. Such scheme is called "strongly coupled", and would provide the physical assimilation with both faster and greater impact on the biogeochemical model skill, and vice versa. Future work will use the improved physical–biogeochemical coupling in the two-way coupled model to inform the development of the data assimilation scheme to include such strong coupling in our operational system.

CRediT authorship contribution statement

Jozef Skákala: Conceptualization, Formal analysis, Investigation, Methodology, Software, Validation, Visualization, Writing - original draft, Writing - review & editing. **Jorn Bruggeman:** Funding acquisition, Software, Supervision. **David Ford:** Conceptualization, Software, Supervision, Writing - original draft, Writing - review & editing. **Sarah Wakelin:** Software, Writing - review & editing. **Anıl Akpınar:** Data curation, Writing - original draft. **Tom Hull:** Data curation, Writing - original draft. **Jan Kaiser:** Data curation, Writing - original draft. **Benjamin R. Loveday:** Data curation, Writing - original draft, Writing - review & editing. **Enda O'Dea:** Supervision. **Charlotte A.J. Williams:** Data curation, Writing - original draft. **Stefano Ciavatta:** Funding acquisition, Project administration, Writing - original draft.

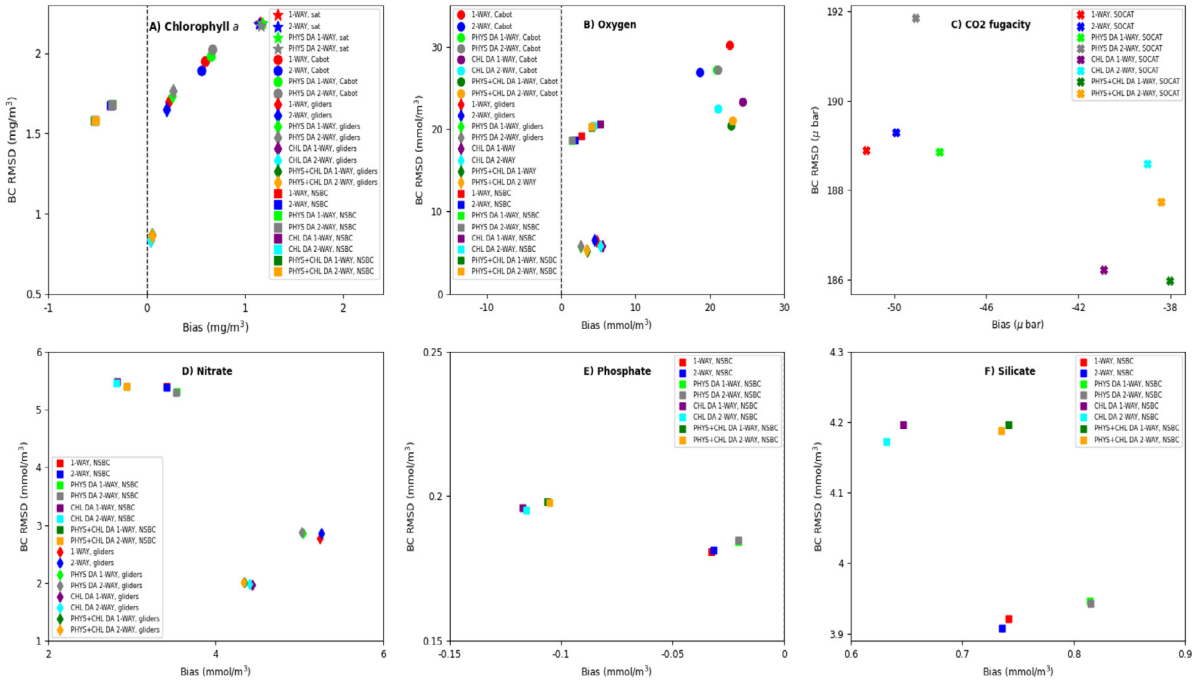

Fig. 10. Skill of the different model simulations to represent chlorophyll *a* (mg/m^3, panel A), oxygen (mmol/m^3, panel B), CO_2 fugacity (μ bar, panel C), nitrate (mmol/m^3, panel D), phosphate (mmol/m^3, panel E) and silicate (mmol/m^3, panel F) concentrations. The skill is measured by bias (x-axis, Eq. (2)) and BC RMSD (y-axis, Eq. (3)). The skill is evaluated for the full year 2018. The different simulations are represented by different colours: 1-WAY (red), 2-WAY (blue), CHL DA 1-WAY (purple), CHL DA 2-WAY (cyan), PHYS DA 1-WAY (lime), PHYS DA 2-WAY (grey), PHYS+CHL DA 1-WAY (green) and PHYS+CHL DA 2-WAY (orange). The different markers show comparison with different data-sets: the star stands for the satellite ocean colour data, the circle for the Cabot glider observations, the diamond for the remaining available glider observations (the 2018 AlterEco mission without Cabot), the cross for the SOCAT data and the square for the NSBC climatological data-set.

Declaration of competing interest

The authors declare that they have no known competing financial interests or personal relationships that could have appeared to influence the work reported in this paper.

Acknowledgements

This work was supported by a Natural Environment Research Council (NERC) funded project of the Marine Integrated Autonomous Observing Systems (MIAOS) programme: Combining Autonomous observations and Models for Predicting and Understanding Shelf seas (CAMPUS). It also benefitted from another NERC funded project Alternative Framework to Assess Marine Ecosystem Functioning in Shelf Seas (AlterECO, http://projects.noc.ac.uk/altereco/), grant no. NE/P013899/1. The work also benefited from the Copernicus Marine Environment Monitoring Service (CMEMS) funded projects OPTIcal data Modelling and Assimilation (OPTIMA) and NOWMAPS. Furthermore, this work was also partially funded by the SEAMLESS project, which received funding from the European Union's Horizon 2020 research and innovation programme under grant agreement No. 101004032. We would like to thank Dawn Ashby for drawing the schematic Fig. 1. The ocean colour data were provided by the European Space Agency Climate Initiative "Ocean Color" (https://esa-oceancolour-cci.org/). The glider data used in the study (http://dx.doi.org/10.5285/b57d215e-065f-7f81-e053-6c86abc01a82 and http://dx.doi.org/10.5285/b58e83f0-d8f3-4a83-e053-6c86abc0bbb5) are publicly available on https://www.bodc.ac.uk/data/published_data_library/catalogue/. We also used L4 time series for chlorophyll *a* concentrations provided by the Western Channel Observatory (https://www.westernchannelobservatory.org.uk/). The model was forced by the atmospheric ERA5 product of The European Centre for Medium-Range Weather Forecasts (ECMWF, https://www.ecmwf.int/). The river forcing data used by the model were prepared by Sonja van Leeuwen and Helen Powley as part of UK Shelf Seas Biogeochemistry programme (contract no. NE/K001876/1) of the NERC and the Department for Environment Food and Rural Affairs (DEFRA). We acknowledge use of the MONSooN system, a collaborative facility supplied under the Joint Weather and Climate Research Programme, a strategic partnership between the Met Office and the NERC. The different outputs for the free run simulations and reanalyses are stored on the MONSooN storage facility MASS and can be obtained upon request.

Appendix A. Supplementary data

Supplementary material related to this article can be found online at https://doi.org/10.1016/j.ocemod.2022.101976.

References

Artioli, Y., Blackford, J.C., Butenschön, M., Holt, J.T., Wakelin, S.L., Thomas, H., Borges, A.V., Allen, J.I., 2012. The carbonate system in the north sea: Sensitivity and model validation. J. Mar. Syst. 102, 1–13.

Baird, M.E., Timko, P.G., Wu, L., 2007. The effect of packaging of chlorophyll within phytoplankton and light scattering in a coupled physical–biological ocean model. Mar. Freshwater Res. 58 (10), 966–981.

Baretta, J., Ebenhöh, W., Ruardij, P., 1995. The European regional seas ecosystem model, a complex marine ecosystem model. Neth. J. Sea Res. 33 (3–4), 233–246.

Baretta-Bekker, J.G., Baretta, J.W., Ebenhöh, W., 1997. Microbial dynamics in the marine ecosystem model ERSEM II with decoupled carbon assimilation and nutrient uptake. J. Sea Res. 38 (3–4), 195–211.

Beaton, A.D., Cardwell, C.L., Thomas, R.S., Sieben, V.J., Legiret, F.-E., Waugh, E.M., Statham, P.J., Mowlem, M.C., Morgan, H., 2012. Lab-on-chip measurement of nitrate and nitrite for in situ analysis of natural waters. Environ. Sci. Technol. 46 (17), 9548–9556.

Behrenfeld, M.J., Boss, E.S., 2018. Student's tutorial on bloom hypotheses in the context of phytoplankton annual cycles. Global Change Biol. 24 (1), 55–77.

Birchill, A., Clinton-Bailey, G., Hanz, R., Mawji, E., Cariou, T., White, C., Ussher, S., Worsfold, P., Achterberg, E.P., Mowlem, M., 2019. Realistic measurement uncertainties for marine macronutrient measurements conducted using gas segmented flow and lab-on-chip techniques. Talanta 200, 228–235.

Blackford, J.C., 1997. An analysis of benthic biological dynamics in a north sea ecosystem model. J. Sea Res. 38 (3–4), 213–230.

Bloom, S.C., Takacs, L.L., Da Silva, A.M., Ledvina, D., 1996. Data assimilation using incremental analysis updates. Mon. Weather Rev. 124 (6), 1256–1271.

Borges, A.V., Schiettecatte, L.S., Abril, G., Delille, B., Gazeau, F., 2006. Carbon dioxide in European coastal waters. Estuar. Coast. Shelf Sci. 70 (3), 375–387.

Bruggeman, J., Bolding, K., 2014. A general framework for aquatic biogeochemical models. Environ. Model. Softw. 61, 249–265.

Bruggeman, J., Bolding, K., 2020. Framework for aquatic biogeochemical models. http://dx.doi.org/10.5281/zenodo.3817997.

Butenschön, M., Clark, J., Aldridge, J.N., Allen, J.I., Artioli, Y., Blackford, J., Bruggeman, J., Cazenave, P., Ciavatta, S., Kay, S., et al., 2016. Ersem 15.06: a generic model for marine biogeochemistry and the ecosystem dynamics of the lower trophic levels. Geosci. Model Dev. 9 (4), 1293–1339.

Campbell, J.W., 1995. The lognormal distribution as a model for bio-optical variability in the sea. J. Geophys. Res. Ocean. 100 (C7), 13237–13254.

Charlson, R.J., Lovelock, J.E., Andreae, M.O., Warren, S.G., 1987. Oceanic phytoplankton, atmospheric sulphur, cloud albedo and climate. Nature 326 (6114), 655–661.

Edwards, A.M., Wright, D.G., Platt, T., 2004. Biological heating effect of a band of phytoplankton. J. Mar. Syst. 49 (1–4), 89–103.

Ford, D., 2021. Assimilating synthetic biogeochemical-argo and ocean colour observations into a global ocean model to inform observing system design. Biogeosciences 18 (2), 509–534.

Ford, D., Kay, S., McEwan, R., Totterdell, I., Gehlen, M., 2018. Marine biogeochemical modelling and data assimilation for operational forecasting, reanalysis, and climate research. New Front. Oper. Oceanogr. 625–652.

Ford, D.A., van der Molen, J., Hyder, K., Bacon, J., Barciela, R., Creach, V., McEwan, R., Ruardij, P., Forster, R., 2017. Observing and modelling phytoplankton community structure in the North Sea. Biogeosciences 14 (6), 1419–1444.

Garcia, H.E., Locarnini, R.A., Boyer, T.P., Antonov, J.I., Baranova, O.K., Zweng, M.M., Reagan, J.R., Johnson, D.R., Mishonov, A.V., Levitus, S., 2013. World ocean atlas 2013. Volume 4, dissolved inorganic nutrients (phosphate, nitrate, silicate).

Gehlen, M., Barciela, R., Bertino, L., Brasseur, P., Butenschön, M., Chai, F., Crise, A., Drillet, Y., Ford, D., Lavoie, D., et al., 2015. Building the capacity for forecasting marine biogeochemistry and ecosystems: recent advances and future developments. J. Oper. Oceanogr. 8 (sup1), s168–s187.

Geider, R.J., MacIntyre, H.L., Kana, T.M., 1997. Dynamic model of phytoplankton growth and acclimation: responses of the balanced growth rate and the chlorophyll a: carbon ratio to light, nutrient-limitation and temperature. Mar. Ecol. Prog. Ser. 148, 187–200.

Good, S.A., Martin, M.J., Rayner, N.A., 2013. EN4: QUality controlled ocean temperature and salinity profiles and monthly objective analyses with uncertainty estimates. J. Geophys. Res. Ocean. 118 (12), 6704–6716.

Goodliff, M., Bruening, T., Schwichtenberg, F., Li, X., Lindenthal, A., Lorkowski, I., Nerger, L., 2019. Temperature assimilation into a coastal ocean-biogeochemical model: assessment of weakly and strongly coupled data assimilation. Ocean Dyn. 69 (10), 1217–1237.

Graham, J.A., O'Dea, E., Holt, J., Polton, J., Hewitt, H.T., Furner, R., Guihou, K., Brereton, A., Arnold, A., Wakelin, S., et al., 2018. AMM15: A new high-resolution NEMO configuration for operational simulation of the European north-west shelf. Geosci. Model Dev. 11 (2), 681–696.

Gregg, W.W., Casey, N.W., 2007. Modeling coccolithophores in the global oceans. Deep Sea Res. Part II: Top. Stud. Oceanogr. 54 (5–7), 447–477.

Gregg, W.W., Casey, N.W., 2009. Skill assessment of a spectral ocean–atmosphere radiative model. J. Mar. Syst. 76 (1–2), 49–63.

Gregg, W.W., Rousseaux, C.S., 2016. Directional and spectral irradiance in ocean models: effects on simulated global phytoplankton, nutrients, and primary production. Front. Mar. Sci. 3, 240.

Heinze, C., Gehlen, M., 2013. Modeling ocean biogeochemical processes and the resulting tracer distributions. In: International Geophysics. vol. 103, Elsevier, pp. 667–694.

Henson, S.A., Dunne, J.P., Sarmiento, J.L., 2009. Decadal variability in north atlantic phytoplankton blooms. J. Geophys. Res. Ocean. 114 (C4).

Hinrichs, I., Gouretski, V., Pätch, J., Emeis, K., Stammer, D., 2017. North Sea biogeochemical climatology. Universität Hamburg.

Huisman, J.E.F., van Oostveen, P., Weissing, F.J., 1999. Critical depth and critical turbulence: two different mechanisms for the development of phytoplankton blooms. Limnol. Oceanogr. 44 (7), 1781–1787.

Jahnke, R.A., 2010. Global synthesis. In: Carbon And Nutrient Fluxes In Continental Margins. Springer, pp. 597–615.

Jin, Z., Charlock, T.P., Smith Jr., W.L., Rutledge, K., 2004. A parameterization of ocean surface albedo. Geophys. Res. Lett. 31 (22).

Jochum, M., Yeager, S., Lindsay, K., Moore, K., Murtugudde, R., 2010. Quantification of the feedback between phytoplankton and ENSO in the community climate system model. J. Clim. 23 (11), 2916–2925.

Kay, S., McEwan, R., Ford, D., 2019. North west European shelf production centre NORTHWESTSHELF_ANALYSIS_FORECAST_BIO_004_011, quality information document. Copernicus Mar. Environ. Monit. Serv.

Key, R.M., Olsen, A., van Heuven, S., Lauvset, S.K., Velo, A., Lin, X., Schirnick, C., Kozyr, A., Tanhua, T., Hoppema, M., et al., 2015. Global Ocean Data Analysis Project, Version 2 (GLODAPv2). Carbon Dioxide Information Analysis Center, Oak Ridge Nat Lab.

King, R.R., While, J., Martin, M.J., Lea, D.J., Lemieux-Dudon, B., Waters, J., O'Dea, E., 2018. Improving the initialisation of the met office operational shelf-seas model. Ocean Model. 130, 1–14.

Lauvset, S.K., Key, R.M., Olsen, A., van Heuven, S., Velo, A., Lin, X., Schirnick, C., Kozyr, A., Tanhua, T., Hoppema, M., et al., 2016. A new global interior ocean mapped climatology: The 1× 1 glodap version 2. Earth Syst. Sci. Data 8, 325–340.

Leles, S.G., Polimene, L., Bruggeman, J., Blackford, J., Ciavatta, S., Mitra, A., Flynn, K.J., 2018. Modelling mixotrophic functional diversity and implications for ecosystem function. J. Plankton Res. 40 (6), 627–642.

Lengaigne, M., Menkes, C., Aumont, O., Gorgues, T., Bopp, L., André, J.-M., Madec, G., 2007. Influence of the oceanic biology on the tropical Pacific climate in a coupled general circulation model. Clim. Dynam. 28 (5), 503–516.

Lenhart, H.-J., Mills, D.K., Baretta-Bekker, H., Van Leeuwen, S.M., Van Der Molen, J., Baretta, J.W., Blaas, M., Desmit, X., Kühn, W., Lacroix, G., et al., 2010. Predicting the consequences of nutrient reduction on the eutrophication status of the north sea. J. Mar. Syst. 81 (1–2), 148–170.

Lovelock, J., 1979. Gaia: A New Look At Life On Earth. Oxford Paperbacks.

Lovelock, J., 2000. The Ages Of Gaia: A Biography Of Our Living Earth. Oxford University Press, USA.

Lovelock, J.E., Maggs, R., Rasmussen, R., 1972. Atmospheric dimethyl sulphide and the natural sulphur cycle. Nature 237 (5356), 452–453.

Lutz, M.J., Caldeira, K., Dunbar, R.B., Behrenfeld, M.J., 2007. Seasonal rhythms of net primary production and particulate organic carbon flux to depth describe the efficiency of biological pump in the global ocean. J. Geophys. Res. Ocean. 112 (C10).

Madec, G., et al., 2015. NEMO ocean engine. Institut Pierre-Simon Laplace.

Manizza, M., Le Quéré, C., Watson, A.J., Buitenhuis, E.T., 2005. Bio-optical feedbacks among phytoplankton, upper ocean physics and sea-ice in a global model. Geophys. Res. Lett. 32 (5).

Marine Systems Modelling Group, P.M.L., 2020. European regional seas ecosystem model. http://dx.doi.org/10.5281/zenodo.3817997.

Marzeion, B., Timmermann, A., Murtugudde, R., Jin, F.-F., 2005. Biophysical feedbacks in the tropical Pacific. J. Clim. 18 (1), 58–70.

Mogensen, K., Balmaseda, M., Weaver, A., Martin, M., Vidard, A., 2009. Nemovar: A variational data assimilation system for the NEMO ocean model. ECMWF Newsl. 120, 17–22.

Mogensen, K., Balmaseda, M.A., Weaver, A., et al., 2012. The NEMOVAR ocean data assimilation system as implemented in the ECMWF ocean analysis for System 4. ECMWF Reading.

Morel, A., 1988. Optical modeling of the upper ocean in relation to its biogenous matter content (case I waters). J. Geophys. Res. Ocean. 93 (C9), 10749–10768.

O'Dea, E., Arnold, A., Edwards, K., Furner, R., Hyder, P., Martin, M., Siddorn, J., Storkey, D., While, J., Holt, J., et al., 2012. An operational ocean forecast system incorporating NEMO and SST data assimilation for the tidally driven European north-west shelf. J. Oper. Oceanogr. 5 (1), 3–17.

O'Dea, E., Furner, R., Wakelin, S., Siddorn, J., While, J., Sykes, P., King, R., Holt, J., Hewitt, H., 2017. The CO5 configuration of the 7 km atlantic margin model: large-scale biases and sensitivity to forcing, physics options and vertical resolution. Geosci. Model Dev. 10 (8), 2947.

Oschlies, A., 2004. Feedbacks of biotically induced radiative heating on upper-ocean heat budget, circulation, and biological production in a coupled ecosystem-circulation model. J. Geophys. Res. Ocean. 109 (C12).

Pauly, D., Christensen, V., Guénette, S., Pitcher, T.J., Sumaila, U.R., Walters, C.J., Watson, R., Zeller, D., 2002. Towards sustainability in world fisheries. Nature 418 (6898), 689.

Riebesell, U., Körtzinger, A., Oschlies, A., 2009. Sensitivities of marine carbon fluxes to ocean change. Proc. Natl. Acad. Sci. 106 (49), 20602–20609.

Sathyendranath, S., Brewin, R.J., Brockmann, C., Brotas, V., Calton, B., Chuprin, A., Cipollini, P., Couto, A.B., Dingle, J., Doerffer, R., et al., 2019. An ocean-colour time series for use in climate studies: The experience of the ocean-colour climate change initiative (OC-CCI). Sensors 19 (19), 4285.

Sathyendranath, S., Gouveia, A.D., Shetye, S.R., Ravindran, P., Platt, T., 1991. Biological control of surface temperature in the arabian sea. Nature 349 (6304), 54.

Schwinger, J., Tjiputra, J., Goris, N., Six, K.D., Kirkevåg, A., Seland, Ø., Heinze, C., Ilyina, T., 2017. Amplification of global warming through pH dependence of DMS production simulated with a fully coupled earth system model. Biogeosciences 14 (15), 3633.

Siddorn, J.R., Furner, R., 2013. An analytical stretching function that combines the best attributes of geopotential and terrain-following vertical coordinates. Ocean Model. 66, 1–13.

Simonot, J.-y., Dollinger, E., Le Treut, H., 1988. Thermodynamic-biological-optical coupling in the oceanic mixed layer. J. Geophys. Res. Ocean. 93 (C7), 8193–8202.

Six, K.D., Kloster, S., Ilyina, T., Archer, S.D., Zhang, K., Maier-Reimer, E., 2013. Global warming amplified by reduced sulphur fluxes as a result of ocean acidification. Nature Clim. Change 3 (11), 975–978.

Skákala, J., Bruggeman, J., Brewin, R.J., Ford, D.A., Ciavatta, S., 2020. Improved representation of underwater light field and its impact on ecosystem dynamics: a study in the north sea. J. Geophys. Res. Ocean. e2020JC016122.

Skákala, J., Ford, D., Brewin, R.J., McEwan, R., Kay, S., Taylor, B., de Mora, L., Ciavatta, S., 2018. The assimilation of phytoplankton functional types for operational forecasting in the northwest European shelf. J. Geophys. Res. Ocean. 123 (8), 5230–5247.

Skákala, J., Ford, D.A., Bruggeman, J., Hull, T., Kaiser, J., King, R.R., Loveday, B.R., Palmer, M.R., Smyth, T.J., Williams, C.A.J., Ciavatta, S., 2021. Towards a multi-platform assimilative system for ocean biogeochemistry. Journal of Geophysical Research: Oceans 126 (4).

Smyth, T.J., Allen, I., Atkinson, A., Bruun, J.T., Harmer, R.A., Pingree, R.D., Widdicombe, C.E., Somerfield, P.J., 2014. Ocean net heat flux influences seasonal to interannual patterns of plankton abundance. PLoS One 9 (6).

Smyth, T.J., Artioli, Y., 2010. Global inherent optical properties from SeaWiFS data. Plymouth Marine Laboratory, http://dx.doi.org/10.1594/PANGAEA.741913.

Storkey, D., Blockley, E.W., Furner, R., Guiavarc'h, C., Lea, D., Martin, M., Barciela, R.M., Hines, A., Hyder, P., Siddorn, J.R., 2010. Forecasting the ocean state using NEMO: The new FOAM system. J. Oper. Oceanogr. 3 (1), 3–15.

Sweeney, C., Gnanadesikan, A., Griffies, S.M., Harrison, M.J., Rosati, A.J., Samuels, B.L., 2005. Impacts of shortwave penetration depth on large-scale ocean circulation and heat transport. J. Phys. Oceanogr. 35 (6), 1103–1119.

Taylor, J.R., Ferrari, R., 2011. Shutdown of turbulent convection as a new criterion for the onset of spring phytoplankton blooms. Limnol. Oceanogr. 56 (6), 2293–2307.

Turner, A., Joshi, M., Robertson, E., Woolnough, S., 2012. The effect of arabian sea optical properties on SST biases and the south Asian summer monsoon in a coupled GCM. Clim. Dynam. 39 (3–4), 811–826.

Vincent, A.G., Pascal, R.W., Beaton, A.D., Walk, J., Hopkins, J.E., Woodward, E.M.S., Mowlem, M., Lohan, M.C., 2018. Nitrate drawdown during a shelf sea spring bloom revealed using a novel microfluidic in situ chemical sensor deployed within an autonomous underwater glider. Mar. Chem. 205, 29–36.

Waniek, J.J., 2003. The role of physical forcing in initiation of spring blooms in the northeast atlantic. J. Mar. Syst. 39 (1–2), 57–82.

Waters, J., Lea, D.J., Martin, M.J., Mirouze, I., Weaver, A., While, J., 2015. Implementing a variational data assimilation system in an operational 1/4 degree global ocean model. Q. J. R. Meteorol. Soc. 141 (687), 333–349.

While, J., Martin, M.J., 2019. Variational bias correction of satellite sea-surface temperature data incorporating observations of the bias. Q. J. R. Meteorol. Soc. 145 (723), 2733–2754.

Wilson, T.W., Ladino, L.A., Alpert, P.A., Breckels, M.N., Brooks, I.M., Browse, J., Burrows, S.M., Carslaw, K.S., Huffman, J.A., Judd, C., et al., 2015. A marine biogenic source of atmospheric ice-nucleating particles. Nature 525 (7568), 234–238.

Zhai, L., Tang, C., Platt, T., Sathyendranath, S., 2011. Ocean response to attenuation of visible light by phytoplankton in the Gulf of St. Lawrence. J. Mar. Syst. 88 (2), 285–297.